

# INDUCTION MICROTRON WITH 90 OR 180 DEGREES BENDING MAGNETS FOR GIANT CLUSTER ION\*

Taufik<sup>1†</sup>, The Graduate University of Advanced Studies, Tsukuba 305-0801, Japan

<sup>1</sup>also at High Energy Accelerator Research Organization, Accelerator Laboratory, Tsukuba 305-0801, Japan

T. Adachi, K. Takayama, K. Okamura, M. Wake, High Energy Accelerator Research Organization, Accelerator Laboratory, Tsukuba 305-0801, Japan

## Abstract

Two types of induction microtron to accelerate giant cluster ions such as C-60 or Si-100 have been studied. They utilize two 180 degrees bending magnets and four 90 degrees bending magnets, respectively. It is characteristic that these bending magnets have the reverse filed strip at the open entrance to assist the orbit stability. Both induction microtrons will employ induction acceleration. The paper will describe some aspects of their beam dynamics and compare both types. A prototype bending magnet with this reverse field strip has been assembled recently. Its characteristic features are discussed.

## INTRODUCTION

Induction microtron for giant cluster ions has been under extensive study at KEK [1]. It is a unique as a repeated accelerator of giant cluster ions. The microtron will make it possible to accelerate giant cluster ions beyond the tandem accelerator energy level. There are two possible scenario of the microtron employing two 180 degrees bending magnets and four 90 degrees bending magnets. The former has been proposed in Reference 1. Since then, extensive design studies have been carried out at KEK. It has been found out through the studies that the time-varying quadrupole focusing and steering correction are inevitable to maintain the orbit stability. For the comparison, the latter has been examined. Its specific feature that the injection/exit angle to the bending magnets is always zero can notably relax various problems associated with the stability, which are main issues in the former scheme. Meanwhile, the 180 degrees bending scheme demands a large size of magnet. Apparently, this is a crucial figure of demerit. The next section will summarize the properties in a comparison of these schemes.

A prototype 90 degrees bending magnet with the reverse filed strip has been assembled in order to confirm an idea where a single set of excitation coils can generate the main bending fields and inversed fields induced by core saturation. Its field measurement has been carried out. The principle has been justified. Meanwhile, a crucial issue is identified how the field uniformity in the longitudinal direction is realized and an importance to protect the gap modification caused by the attractive magnetic force is recognized.

\* Work supported by Grants-In-Aid for Scientific Research (B) (KAKENHI No. 15H03589) and for Exploratory Research (KAKENHI No. 17K19091).

† taufikis@post.kek.jp

## POSSIBLE SCHEME OF MICROTRON

### Outline of 180 Degrees and 90 Degrees Bend Microtrons

Here, acceleration of C60<sup>10+</sup> ion up to 144 MeV is considered as a typical example.

The 180 degrees bend microtron consists of two 180 degrees bending magnets with inverse field for focusing in the vertical plane. In the horizontal plane, a quadrupole magnet (QF) stabilizes an orbit, since the 180 degrees bending field simply plays a role of  $\pi$ -section. Five induction cells accelerate ions by 50 kV/turn, so that the 2 MeV ion reaches its maximum up to 286 turns. Lattice configuration and the beam orbit up to 286 turns are shown in Fig. 1, where the color distinguishes turn number. Transverse beam envelopes with emittance of 100  $\pi$ mm.mrad up to 286 turns are shown in Fig. 2.

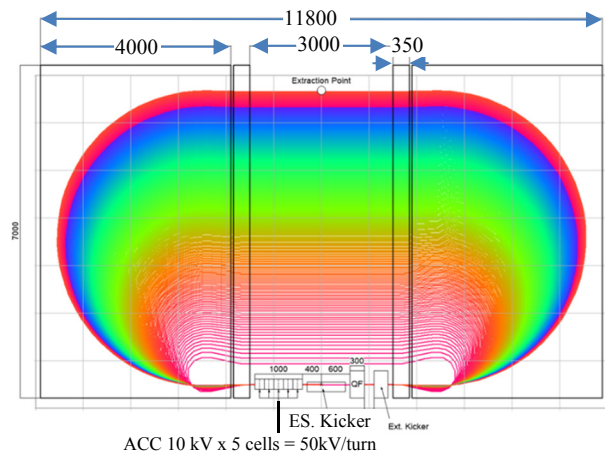


Figure 1: Lattice configuration and the beam orbit of the 180 degrees bend microtron.

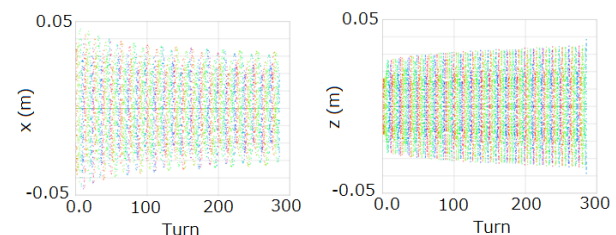


Figure 2: Beam envelopes at the extraction point up to 286 turns.

The 90 degrees bend microtron consists of four 90 degrees bending magnets and four sets of quadrupole doublets (QF and QD). Since large injection/exit (edge) angle (~45 degrees) causes serious defocusing effect in the vertical plane, an inverse field strip is placed at the entrance of the bending magnet, an inverse magnet for edge angle reduction. Even if the edge angle is reduced, defocusing effect in the vertical plane is still serious. The gradient field is added to the main bending field. Thus, beam transverse motion is stabilized by the fixed inverse field strip and main gradient field, and time varying quadrupole field. Gradient fields of the quadrupole magnets are ramped to satisfy the stability condition of the transverse motion every turn.

An induction cell accelerates ions by 10 kV/turn, so that the 10 MeV ion achieves its maximum up to 1340 turns. Lattice configuration and the beam orbit up to 1340 turns are shown in Fig. 3.

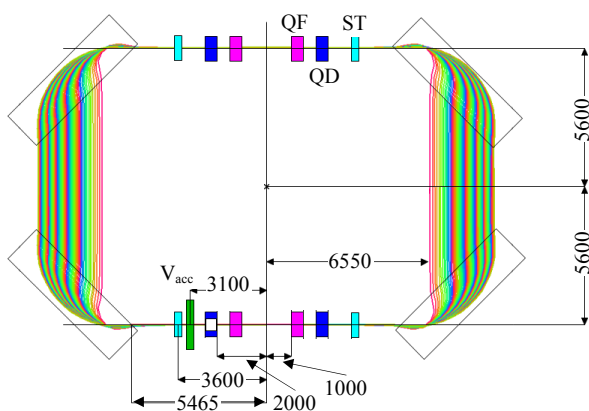


Figure 3: Lattice configuration and the beam orbit of the 90 degrees bend microtron.

Transverse beam envelopes with emittance of  $1 \pi\text{mm.mrad}$  are shown in Fig. 4.

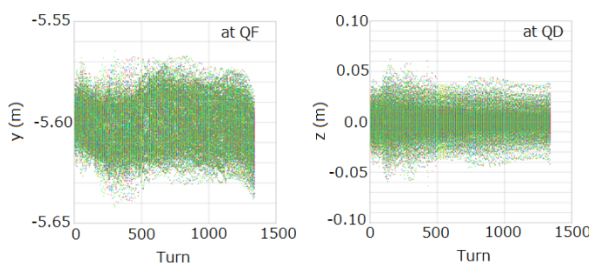


Figure 4: Beam envelopes at QF or QD up to 1340 turns.

### Advantage and Disadvantage

As shown in Fig. 5, the ring size of the 180 degrees bend microtron is smaller than the 90 degrees bend microtron. Other characteristics of two schemes are summarized in Table 1. The 180 degrees bend microtron can accommodate of a large emittance beam because of the notably relaxed orbit stability condition.

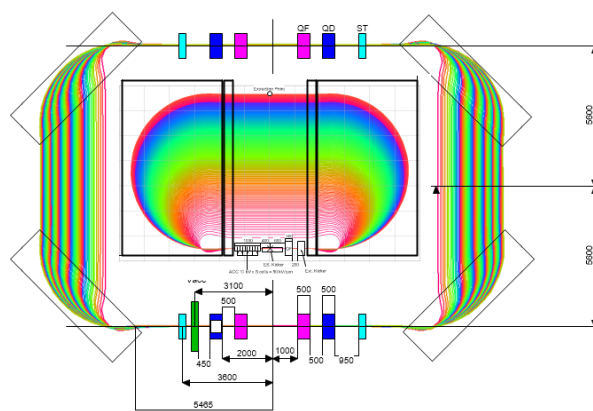


Figure 5: Comparison of ring sizes of two schemes.

Table 1: Characteristics of Two Schemes of a Microtron

	180 degree bend	90 degree bend
Weight of the main magnet (ton)	700	200
Main bending field (T)	1.5	1.5 (gradient field)
Quadrupole field (T/m)	0.1 (QF) fixed	1.0 → 4.0 (QF), 1.0 → 4.5 (QD)
Transverse acceptance ( $\pi\text{mm.mrad}$ )	100	1.0
Injection energy (MeV)	2.0	10.0

Even if there are many attractive characteristics, the 180 degrees bend microtron seems not to be practical because of huge weight and size of its main magnet. However, it can be available for a lower energy microtron like an injector. Figure 6 shows an example of an injector microtron, which accelerate  $\text{C}_{60}^{10+}$  from 2 MeV to 12 MeV.

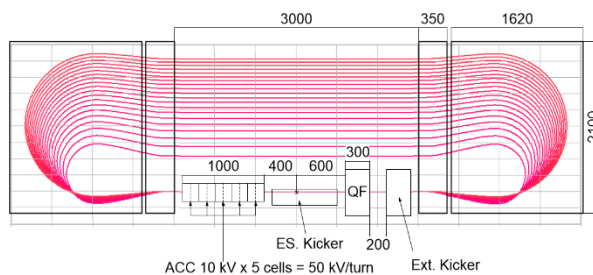


Figure 6: Example of an injector microtron.

## KEY DEVICE OF THE 90 DEGREES MICROTRON

### Bending Magnet with the Reversed Field Strip and Gradient

As mentioned earlier, the vertical stability is crucial in the 90 degrees bend microtron. Employing the reverse field strip in the front end of the bending magnet provides additional edge vertical focusing as shown in Fig. 7. A net vertical focusing in the banding magnet can be acquired with this edge focusing and gradient field in the main field region.

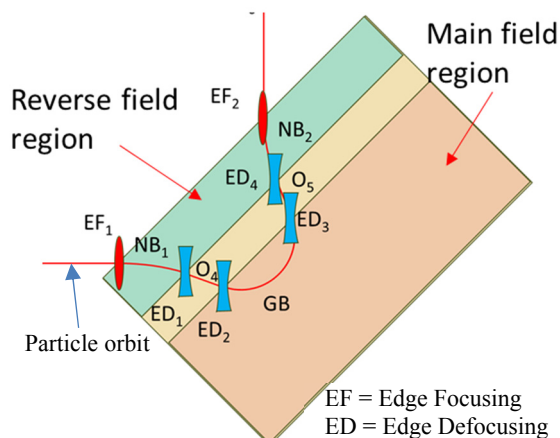


Figure 7: Vertical edge focusing in the 90° induction microtron bending magnet.

The 90 degrees bending magnet, which generates the reverse field and gradient field simultaneously by using single set of coils, was designed. The reverse field is generated in the front end gap and the gradient field is generated in the main field region as shown in Fig. 8. The reverse field will be generated when the magnetic flux density of the main core achieves saturation.

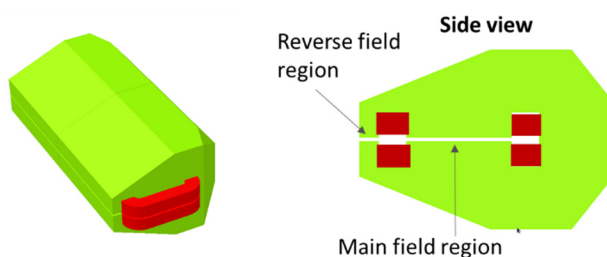


Figure 8: The 90 degrees bending magnet.

Uniformity of the magnetic field in the longitudinal direction is known to be an important issue as extensively discussed in the last conference [2] and elsewhere [3]. Non-uniform magnetic field induces inherent Closed Orbit Distortion (COD) which significantly affects on the stability in the horizontal direction. The uniformity of the magnetic field can be obtained by optimizing the pole shape. This optimization can be carried out by using the 3D numerical code such as ANSYS® or OPERA-Tosca®.

In order to manifest properties of 90 degrees bending magnet, a prototype of the bending magnet with a size of almost one-eighth of the real size design as shown in Fig. 9 was designed and assembled. A curved pole shape along the longitudinal direction is assumed to realize the magnetic field uniformity. The curvature of the pole is decided by using the 4 points spline method. The pole shape and the optimized magnetic field are shown in Fig. 10.

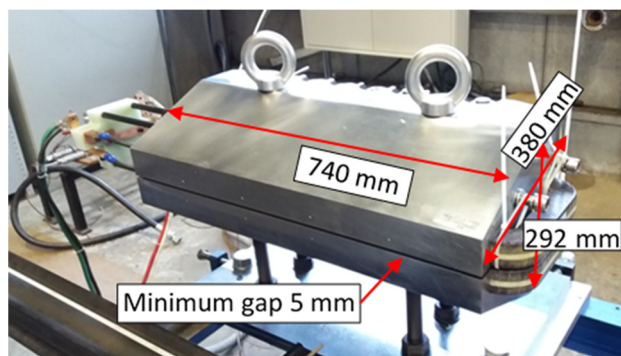


Figure 9: Prototype 90 degrees bending magnet.

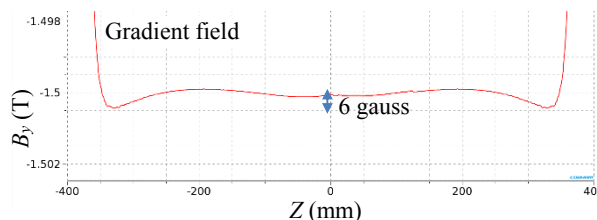
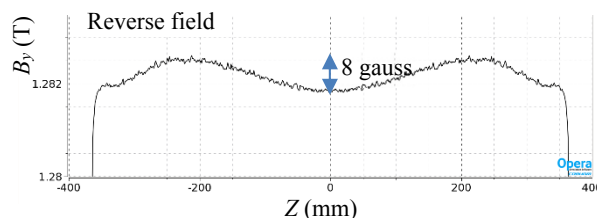
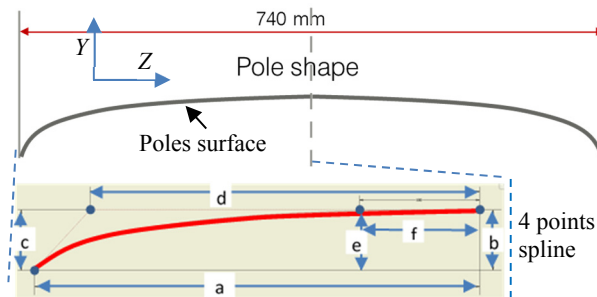


Figure 10: Optimized pole shape and magnetic fields.

### Field Measurement of the Prototype Magnet and Its Analysis

**Gap Size Measurement** The pole shape of the reverse field and main field region were individually measured before assembling of two poles. After assembling, the reverse field pole gap was measured by a micrometer and FARO® gage tools. The measurement results show that the average discrepancy between the design and measurement without excitation is 70 μm in the main field and 120 μm in the reverse field, respectively. Both measurement results using the micrometer and FARO gage are almost consistent.

**Gap Deformation Associated with Excitation** It is found that the gap size is notably deformed with excitation. This deformation is shown as a function of the excitation

current in Fig. 11. The magnitude of gap deformation depends on the bolts torque to screw the upper and bottom cores. The gap deformation due to the magnetic field attraction force can be estimated by Tosca code. Tosca calculation shows a 700  $\mu\text{m}$  gap deformation at 122 A, resulting in field enhancement of 1600 gauss.

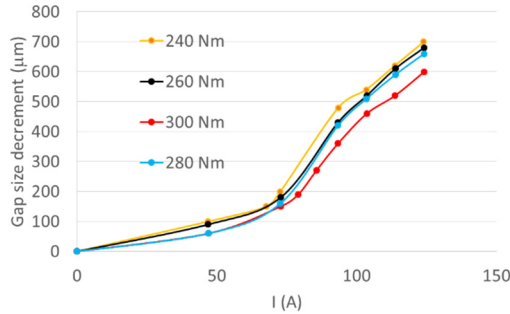


Figure 11: Gap size deformation vs. excitation current.

The magnetic field attraction force ( $F$ ) is written in the following form

$$F = \frac{AB^2}{2\mu_0}, \quad (1)$$

where  $A$  is the pole surface area,  $B$  is the magnetic flux density, and  $\mu_0$  is the permeability in vacuum. By substituting the measured magnetic flux density into Eq. (1),  $F$  at 240 Nm bolt torque is obtained and the observed gap deformation is shown as a function of this  $F$  in Fig. 12.

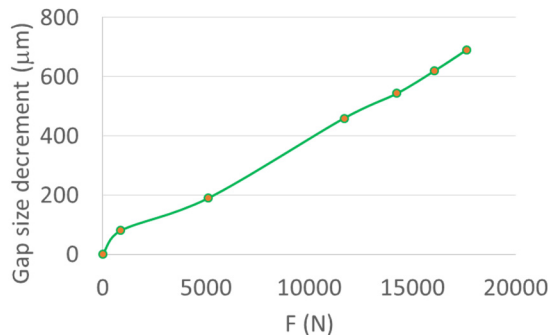


Figure 12: Experimental result of the gap deformation vs. the magnetic attraction force.

**Excitation Curve** Excitation curves of the prototype magnet were measured at the symmetric point on the median plane of the main and reverse field, respectively. The measurement and calculation of the excitation curve are shown in Fig. 13. The magnetic field in the main bending region linearly increases up to some point of the excitation ( $\sim 35 - 40\text{A}$ ) as the coil current increases. Meanwhile, the reverse field linearly increase beyond this threshold current. This feature can be explained as follow: Until the threshold current the resistance of the magnetic circuit between the main gap and main return yoke is below that between the main gap and the front core with the tiny reverse field gap, meanwhile, beyond the threshold current the resistance of

the former magnetic circuit exceeds that of the latter circuit, resulting in appearance of the reverse field in the front gap.

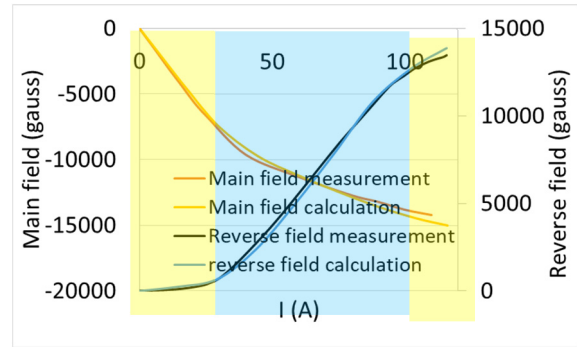


Figure 13: Excitation curve of the bending magnet. The excitation is divided into three regions: in Region I the main field rapidly increases without appearance of the reverse field in the front gap, in Region II both of the main field and reverse field linearly increase, and in Region III the main field seems to be excited below saturation and the reverse field region achieves saturation.

**Magnetic Field Mapping** Field mappings in the X (lateral) and Z (longitudinal) direction were carried out at the full excitation (112.4 A).  $B_y(X,0,0)$  is given as function of  $X$  in the Fig. 14. Figure 14 shows that two opposite magnetic fields are induced in the main field gap and reverse field gap by a single pair of coils, as expected. In the main field gap, the negative gradient field is slightly observed even though the pole was not designed to produce such a field gradient. This field gradient can be attributed to the deformation of the gap size due to the magnetic field attraction force mentioned previously.

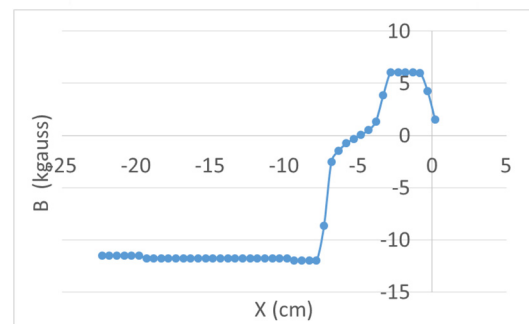
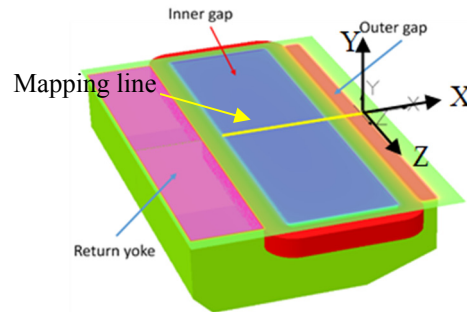


Figure 14: Line mapping in X direction.

$B_y(X,0,Z)$  observed at the coil current of 122.4 A is shown as a function  $Z$  in Fig. 15. It is clear that the peak to

peak of  $B_y$  are in order of 300 gauss which are much bigger than the design value. The discrepancies between the field measurement and the design value can be attributed to the deviation from the designed pole shape.

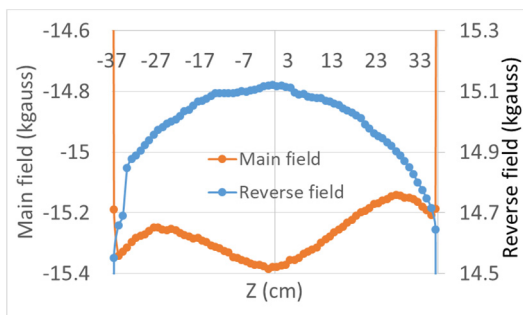
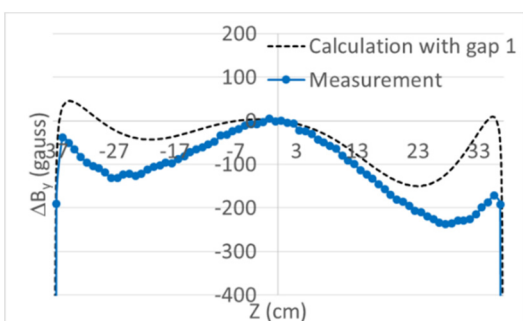
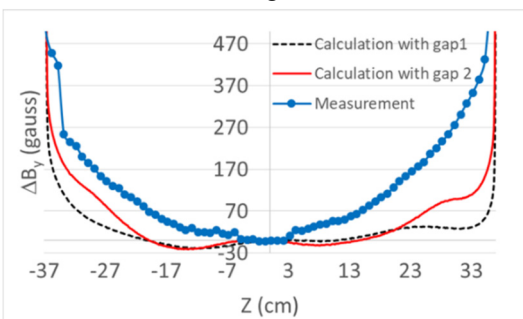


Figure 15: Magnetic field mapping in Z direction.

In order to compare the Tosca calculation and the measurement result, the gap size parameter in the Tosca calculation was modified assuming the actual gap size. Gap 1 that refers to KEK machine shop data and gap 2 that refers to the micrometer measurement data were used in the Tosca calculation. The difference of the magnetic flux density ( $\Delta B_y$ ) on the Z position relative to the center of magnet length ( $Z=0$ ) of the Tosca calculation and measurement result is clear in Fig. 16. The unbalance of the  $\Delta B_y$  may be originated from the non-uniformity along Z of the gap size, which is shown in Fig. 17. However, the discrepancy between calculation and measurement has not been fully understood yet, although the gap deformation may affect the result.



a. Main magnetic field



b. Reversed magnetic field

Figure 16: Magnetic field uniformity in the Z direction.

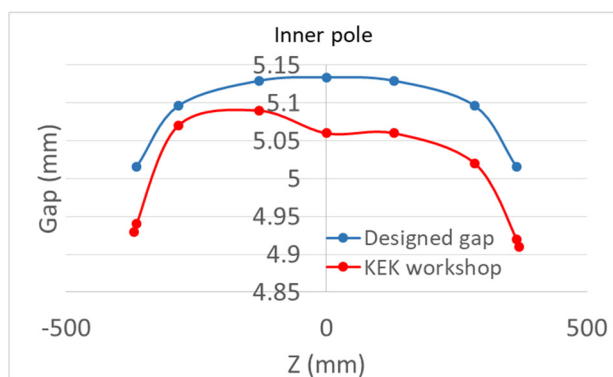


Figure 17: Measured gap size vs. Z.

## SUMMARY

The 90 degrees-bend IM seems to be practical for high energy acceleration of giant cluster ions. However, a combination of 180/90 degrees bend IMs may be attractive as a cascade-type accelerator complex [4]. Their figure of merits should be utilized there. Both IMs are assumed to employ the bending magnet with a reverse field strip. Its prototype magnet has been assembled and tested. An original idea that the change of magnetic resistance in the magnetic flux circuits associated with excitation induces the reverse fields has been confirmed as expected. However important issues such as the pole gap size modification and field non-uniformity in the longitudinal direction, that have to be resolved in a real-size magnet, have been realized through the field measurements.

## ACKNOWLEDGEMENTS

The authors would like to thank N. Higashi for the pole shaping works and pole shape measurement.

## REFERENCES

- [1] K. Takayama, T. Adachi, M. Wake, and K. Okamura, "A race-track-shape fixed field induction accelerator for giant cluster ions", *Phys. Rev. ST Accel Beams*, vol. 18, p. 050101, May 2015, doi: 10.1103/PhysRevSTAB.18.050101
- [2] Taufik, T. Adachi, M. Wake, and K. Takayama, "Lattice design of the 144 MeV induction microtron for C-60", in Proc. of The 14th Annual Meeting of Particle Accelerator Society of Japan (PASJ), Sapporo, Japan, Aug. 2017, paper TUP023, pp. 359-363.
- [3] Taufik, T. Adachi, M. Wake, and K. Takayama, "Beam dynamic of induction microtron", submitted to *Phys. Rev. Accel. & Beams*.
- [4] K. Takayama, "Study on the Main Driver for Giant Cluster Ion Inertial Fusion (G-CLIF)", presented at the 22<sup>nd</sup> International Symposium on Heavy Ion Inertial Fusion (HIF2018), in Daejeon, Korea 20-24 August.